Ab initio characterization of a Ni-related defect in diamond: The W8 center

Thomas Chanier[1] and Adam Gali[1,2]

[1]*Wigner Research Center for Physics and Optics, Hungarian Academy of Sciences, P.O. Box 49, H-1525 Budapest*

[2]*Department of Atomic Physics, Budapest University of Technology and Economics, Budafokiút 8., H-1111 Budapest, Hungary*

(Received 8 March 2013; revised manuscript received 16 April 2013; published 19 June 2013)

We provide *ab initio* characterization of the negatively charged substitutional nickel (Ni_s^-) impurity in diamond using a hybrid density functional calculation. Ni_s^- is shown to carry a spin $S = 3/2$. The calculated hyperfine couplings on this defect support the identification of the W8 electron paramagnetic resonance center with Ni_s^- defect. We unambiguously determine the position of the Ni_s^- acceptor level in the gap. This level is located at about 2.0 eV above the valence band maximum and corresponds to a totally occupied triplet state responsible for the magnetization. We calculated the excited state properties of the defect. Our results may resolve the controversial assignments of Ni_s^- to different optical centers.

DOI: 10.1103/PhysRevB.87.245206 PACS number(s): 71.15.Mb, 61.72.Bb, 71.55.Ht

I. INTRODUCTION

Diamond has developed a lot of interest among the research community due to its potential use in quantum computing applications. Indeed its wide band gap of 5.5 eV allows the existence of a large number of optical spin centers.[1] One of the most studied color center in diamond is the NV center. In the negatively charged state, the NV^- center has a spin $S = 1$ and is responsible for a zero phonon line (ZPL) at 1.945 eV between the $^3A_2$ ground state and the ^3E excited state.[2] The intermediate $^1A_1$ excited state allows for the existence of a spin dependent fluorescence and optical spin initialization and readout,[3–7] and spin manipulation via interaction with a neighboring nitrogen nuclear spin[8,9] or electron spin[10] has been successfully demonstrated. An unwanted property of the NV center is that it predominantly emits light in the phonon side band (95%) even at low temperatures. At room temperature its ZPL intensity is small compared to that of the phonon-assisted band.

Alternative bright color centers in diamond with sharp and nearly temperature independent ZPL are of prime importance that can be potential candidates in quantum information processing related applications. Unlike the case of the NV center, the microscopic origin, the electronic structure and magnetic properties of other potentially important color centers in diamond are much less understood. In this regard, *ab initio* calculations are a powerful tool to provide a clear picture of these defects.

Transition metals in diamond might play an important role as they can form color centers in diamond and can be intentionally doped in diamond. For example, a neutral substitutional Ni impurity has been proposed to form a decoherence free subspace for quantum computing application with spin manipulation done by the application of strain.[11] Ni is present as a diluted impurity in synthetic diamond grown by the high-pressure–high-temperature (HPHT) method using Ni as a solvent catalyst. Ni can also be introduced in the perfect diamond lattice by chemical vapor deposition or ion implantation.[12,13]

Ni is responsible for numerous optical centers in diamond with the most well-known located at 1.4, 2.56, and 3.1 eV.[14] The 1.4 and 2.56 eV centers are both active in luminescence and absorption, whereas the 3.1 eV center is observed only in absorption. The 1.4 eV center has been attributed to interstitial Ni in the positively charged state.[15] The absorption lines at around 3.1 eV have been reported in synthetically grown diamonds using a Ni-containing solvent.[14,16] The 3.1 eV center interacts predominantly with a 26 meV quasilocal vibration.[14] An electron paramagnetic resonance (EPR) study shown that substitutional Ni in the negatively charged state Ni_s^-, or the so-called W8 center, carries a spin $S = 3/2$ with a Landé factor $g = 2.0319$.[17] A photo-EPR measurement shows two thresholds at 2.5 and 3.1 eV in the optical cross section and suggested that the $Ni_s^{0/-}$ acceptor level was located at 3.03 eV above the valence band.[18,19] An optically detected magnetic resonance (ODMR) study measured an isotropic Landé factor g value of 2.032 for the 2.56 eV photoluminescence band, which they attributed to Ni_s^-.[20] On the other hand, the 2.56 eV center shows two quasilocal modes at 24 and 36 meV in the luminescence spectra, which has been attributed to two Ni atoms in clear contradiction with the previous assignment.[14]

In order to clarify this situation, we provide a thorough theoretical characterization of the Ni_s defect by means of a density functional theory calculation. We used first the generalized gradient approximation (GGA) to the exchange correlation functional.[21] We apply this method in the calculation of the vibration modes within the density functional perturbation theory. To correct for the band gap error of the GGA functional, we used the HSE06 range-separated, screened, nonlocal hybrid density functional method.[22,23] In order to check the validity of the HSE06 functional on the defect level in the gap, we carried out further calculations using the G_0W_0 many body perturbation theory method.[24] The HSE06 and G_0W_0 calculations are in good agreement which allow us to conclude about the position of the acceptor level in the gap, with a totally occupied antibonding triplet state located at 2.0 eV above the valence band maximum (VBM). We described also the excited state properties of Ni_s^- within HSE06. Our results indicate that Ni_s^- is responsible for the 3.1 eV absorption line, with an excitation corresponding to the promotion of an electron from the antibonding defect state to the conduction band. The manuscript is organized as follows. In Sec. II we describe the method and present the results in Sec. III. In Sec. IV we discuss our results compared with experiments. Sections V and VI are left for summary and conclusion.

II. METHOD

Plane wave supercell calculations were carried out to model the nickel substitutional defect in diamond by using the VASP5.3 code.[25,26] The projector augmentation wave method[27] allows us to accurately calculate the hyperfine couplings between the electron and nuclear spin. We applied the standard C and Ni PAW potentials[27] from the VASP5.2 database. Ni $3d$ electrons were treated as valence electrons. We calculated the hyperfine tensors for ^{61}Ni and ^{13}C isotopes as implemented in VASP5.3. Our study on well-established defects in semiconductors showed that we can reproduce the measured hyperfine constants.[28] The valence wave functions were expanded by plane waves, where the corresponding kinetic energy cutoff $E_{\text{cut}} = 420$ eV was applied to converge the total energy within a 1 meV precision, whereas a larger cut-off energy $E_{\text{cut}} = 840$ eV was necessary to converge the hyperfine coupling calculations.

We utilized several levels of approximation in the Hamiltonian. We first used the GGA approximation in the parametrization of Perdew-Burke-Ernzerhof (PBE).[21] The geometry were fully relaxed at the PBE level until the forces were less than 0.01 eV/Å. The perfect diamond indirect band gap value calculated within PBE is 4.14 eV lower than the experiment value of 5.48 eV.[29] In order to obtain an accurate electronic structure we either applied the HSE06 screened range-separated hybrid density functional theory[22,23] or GW correction to the PBE functional.[24] In the GW correction, the Green-function G and the screened Coulomb-interaction W were fixed as calculated from the PBE functional, the G_0W_0 method. We applied 2304 conduction bands in these calculations. The calculated indirect band gap of diamond is 5.29 and 5.56 eV by HSE06 and G_0W_0 methods, respectively.

Since we applied several levels of approximation in the Hamiltonian, we fixed the lattice constant in the calculations at the experimental lattice constant of $a = 3.567$ Å.[30] The calculated PBE lattice constant agrees with the experimental one within numerical accuracy, while the HSE06 lattice constant is about 0.6% smaller, thus using the experimental lattice constant in the diamond supercell model is acceptable for both functionals. We applied the 512-atom simple cubic supercell to calculate the electronic structure and hyperfine tensors within Γ point. The computationally demanding G_0W_0 calculations were carried out in a 216-atom supercell with $2 \times 2 \times 2$ Γ-centered k-point mesh. As we will see, the PBE functional reproduces well the ground state properties of the defect. We therefore used this functional for the vibration calculations within a density functional perturbation theory.[31] For this calculation we used a $4 \times 4 \times 4$ Monkhorst-Pack grid.[32] We analyzed the normal modes with the inverse participation ratio method in order to find the quasilocal vibration modes.[33] The localization of the electron wave functions were analyzed by projecting the electron density to the valence atomic orbitals of the constituent atoms by using the projectors of the PAW potentials.

III. RESULTS

We first report on the ground state calculation. We start from the PBE calculations. We obtain a total magnetization of 3.0 μ_B. Due to the tetrahedral symmetry, the Ni $3d$ levels are split into a lower doublet e level and an upper triplet t_2 level. In diamond there is hybridization between the nearest-neighbor (NN) carbon $2p$-derived t_2 levels and the Ni $3d$-derived t_2 levels and the formation of bonding (t_B) and antibonding (t_{AB}) levels.[34] The spin up $t_{AB}^{\uparrow}$ levels are located at 2.2 eV above the VBM and are totally occupied. The spin down $t_{AB}^{\downarrow}$ levels are located at 3.0 eV above the VBM and are totally empty. The Ni-related e levels are located at −1.4 and −1.0 eV for spin up and spin down, respectively, and are strongly localized on Ni. The electronic structure can be explained by a p-d hybridization model (Fig. 1) between the $3d$-derived t_2 levels of Ni in configuration $3d^{10}$ and the $2p$-derived t_2 levels of the NN carbon atoms occupied by three electrons. We checked the occupations of Ni and the NN carbon which are consistent with the model.

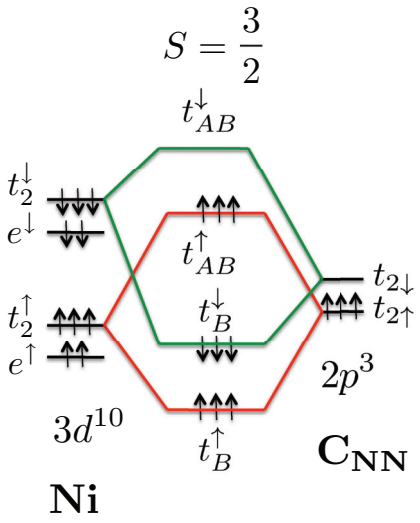

FIG. 1. (Color online) p-d hybridization model for Ni_s^-. The Ni in configuration $3d^{10}$ hybridizes with the nearest-neighbor (NN) C atoms in $2p^3$ configuration.

To correct for the band gap error, we applied the HSE06 calculations. The calculated total magnetization is 3.0 μ_B. The Ni-related $e_{\uparrow}$ ($e_{\downarrow}$) levels are now located at −1.8 (−1.0) eV below the VBM and have a strong $3d$ character localized on Ni. The totally occupied triply degenerated $t_{AB}^{\uparrow}$ is located at 2.0 eV above VBM and is formed primarily of Ni $3d$ and NN carbon $2p$ character. The totally empty triply degenerated $t_{AB}^{\downarrow}$ is located at 4.0 eV above VBM. Due to strong hybridization, this t_{AB} level forms a bound state in the gap[35,36] clearly visible on the spin density plot (Fig. 2). The spin density is mostly localized on the Ni and the NN carbon corresponding to the strong hybridization. We note that there is a nonzero spin density on 12 third-nearest-neighbor carbon atoms ($C_{3^{rd}NN}$). Indeed, the calculated $^{13}C_{3^{rd}NN}$ hyperfine couplings of $A_{xx} = 7.3$; $A_{yy} = 7.2$; $A_{zz} = 10.3$ MHz agree well with the experimental values of $A_{xx} = 7.6$; $A_{yy} = 7.5$; $A_{zz} = 10.7$ MHz.[17] In this experiment they assigned those hyperfine couplings to the next-nearest neighbor which are in fact according to our calculation due to the third NN carbon atoms in agreement with previous theoretical work.[37]

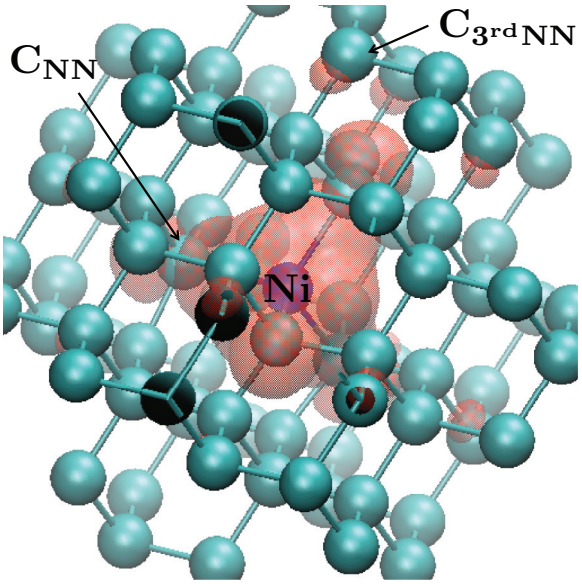

FIG. 2. (Color online) Spin density of the NiC_{511} supercell calculated within the HSE06 approximation. For the sake of visibility we show only atoms within a sphere of radius 5.4 Å around the defect.

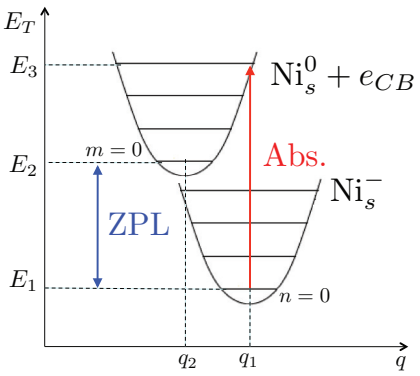

FIG. 3. (Color online) Total energy vs configuration coordinates for the ground state Ni_s^- and the excited state $Ni_s^0 + e_{CB}$ in the Franck-Condon approximation. E_1 and E_3 are the total energy of the ground state and excited state at the relaxed geometry of the ground state and E_2 is the total energy of the excited state at its relaxed geometry. $m = 0$ and $n = 0$ are the lowest phonon levels in each case. The vertical absorption is the total energy difference between the excited state and the ground state at the geometry of the ground state (Abs. $= E_3 - E_1$), whereas for the zero phonon line the excited state is allowed to relax (ZPL $= E_2 - E_1$).

We found that the core polarization contributes to a large extent to the hyperfine values of ^{61}Ni and $^{13}C_{NN}$. We obtain isotropic hyperfine couplings on ^{61}Ni of 18 MHz in agreement with a previous calculation[38] and the experimental values of 18.2 MHz.[17]

We calculated the charge transition level by the following formula:

$$E(q \to q+1) = E_{q+1}^T - E_q^T - \varepsilon_V + \delta_{q+1} - \delta_q, \qquad (1)$$

where E_q^T is the total energy of Ni_s in the charge state q, ε_V is the valence band maximum of the perfect diamond supercell, and δ_q is the charge correction to the total energy. The appropriate charge correction of deep defects is still under debate.[39–45] Our defect belongs to the category of deep states where the 2/3 fraction of the monopole Makov-Payne correction works reliably, thus we adopted this correction: $\delta_q = \frac{2}{3}\frac{q^2\alpha}{2\epsilon L}$ with $\alpha = 2.84$ as the Madelung constant of the simple cubic lattice,[46] $\epsilon = 5.70$ is the dielectric constant of diamond, and $L = 4a$ is the linear dimension of the supercell. For $q = \pm 1$ we obtain $\delta_q = 0.16$. Table I gives the results for GGA and HSE06, both uncorrected and corrected compared with the GGA values from the literature. We note that our GGA values differ from the transition energy of Ref. 38 where they used a 64-atom supercell NiC_{63}. We carried out GGA calculation on the same supercell and noticed that finite size effect is important in this case. Indeed, for NiC_{63}^0, the antibonding $t_{AB}^{\uparrow}$ levels are shifted upwards by 0.5 eV compared to the NiC_{511}^0 $t_{AB}^{\uparrow}$ position of 1.7 eV above the valence band. In this small supercell we also obtain a relatively large dispersion of 0.4 eV. The use of the 512-atom supercell is therefore necessary to obtain the right position of the transition levels. Within the charge corrected HSE06, Ni_s^- is stable for a Fermi energy between 2.36 and 4.66 eV. In midgap or slightly n-type diamond the negative charge state is stable which is a favorable condition in diamond.

TABLE I. Transition level $E(q \to q+1)$ (with respect to the valence band) calculated by GGA, HSE06, and HSE06 + charge correction (HSE06 + CC) compared with the GGA values from Ref. 38 (GGA-R 38), and zero phonon line energies (ZPL). All values are in eV.

Transition	GGA-R 38	GGA	HSE06	HSE06 + CC
$E(+1 \to 0)$	2.6	1.40	1.63	1.46
$E(0 \to -1)$	3.0	2.00	2.20	2.36
$E(-1 \to -2)$	4.0	3.55	4.17	4.66
ZPL	–	2.05	2.88	–

We calculated the vertical absorption and the ZPL corresponding to the transition of an electron from the $t_{AB}^{\uparrow}$ level of Ni_s^- to the conduction band minimum (CBM) $Ni_s^0 + e_{CB}$ (Fig. 3) with the constrained density functional theory method.[47] By promoting an electron from the $t_{AB}^{\uparrow}$ to the CBM, the system becomes Jahn-Teller unstable, thus the excited state reconstructs to C_{1h} symmetry. The HSE06 (GGA) value for the vertical absorption is 3.06 eV (2.15 eV) and the ZPL is 2.88 eV (2.05 eV). We calculated the quasilocal vibration modes in the ground state. We obtain a single mode at 38.4 meV which is triply degenerate.

As mentioned earlier, our results are in contradiction with the photo-EPR results. In order to confirm our prediction, we did G_0W_0 calculations. The antibonding triplet state $t_{AB}^{\uparrow}$ is now located at 2.0 eV above the VBM and is totally occupied, responsible for the total spin $S = 3/2$. The antibonding triplet $t_{AB}^{\downarrow}$ is now at 4.5 eV above VBM and is totally empty. The results are in very good agreement with the HSE06 results.

IV. DISCUSSION

Our results are in contradiction with the interpretation of photo-EPR data.[18,19] In their experiment they measured two thresholds at 2.5 and 3.1 eV in the optical cross section, whereas they determined the position of the acceptor level by a fit[48] to be at 3.03 eV above the valence band. Our calculation shows that the 3.1 eV threshold corresponds to the ionization process $Ni_s^- + h\nu \rightarrow Ni_s^0 + e_{CB}$. This is consistent with the steep increase of the optical cross section marking a very efficient ionization process. Our calculation excludes the 2.5 eV threshold as due solely to Ni_s^-. This threshold might be due to an indirect process obtained by ionizing other nearby defects that affect the optical cross section.

The vacancy model[49] can be applied to the Ni_s^- defect in diamond. In this model the Ni $3d$ levels are located deep in the valence band and totally occupied, and the acceptor t_2 level is formed primarily of the NN carbon t_2 level occupied by three electrons. The multielectron ground state is a quartet $^4A_2$ at the energy $\frac{3\Delta}{4} - \frac{3U}{4}$ and the excited states are doublets $^2T_1$ at $\frac{3\Delta}{4} - \frac{U}{2}$ and two degenerated doublets ^2E and $^2T_2$ at an energy $\frac{3\Delta}{4}$ with Δ as the kinetic energy and U as the on-site Coulomb potential for the carbon $2p$ electrons.[50] The lowest possible transition is between the two excited doublet states $^2T_1$ and $^2T_2$ with a transition energy $\Delta E = U/2$. A transition $\Delta E \sim 2.5$ eV would require an on-site Coulomb potential U of the order of 5 eV, which seems to be realistic. According to this approximation the energy difference between the quartet ground state and the higher doublet excited states would be around 3.7 eV, which is much larger than the ZPL of 3.1 or 2.56 eV Ni-related centers. Thus it seems unlikely that the transition between multiplet doublet states of Ni_s^- can play a role in these Ni-related centers.

Two quasilocal modes of 24 and 36 meV have been measured for the 2.56 eV center in photoluminescence, whereas only one at 26 meV has been found for the 3.1 eV center in absorption.[14] The former belongs to the ground state vibrations, while the latter to the vibration in the excited state. We found here a single triplet mode of 38.4 meV in the ground state of Ni_s^- defect. This finding contradicts the two quasilocal modes of 2.56 eV center. According to the calculations the Ni_s^- defect reconstructs to C_{1h} symmetry in the excited state, where the triplet vibration mode can split and one of them could be strongly visible in the phonon sideband of the absorption.

We argue that our calculated ZPL of 2.88 eV is closer to the 3.065 eV zero-phonon absorption center than to the 2.56 eV ZPL, and the calculated vibration modes also favor the assignment of Ni_s^- defect to the 3.1 eV absorption center. The 3.1 eV center is formed by two ZPL, one at 3.065 eV and the other at 3.076 eV. We can see a conduction band minimum splitting of $\sim$0.01 eV which can explain the two ZPL separated by 11 meV. By this model the 3.1 eV threshold in the photo-EPR measurement of the W8 center can be well accounted for as the $(-1 \rightarrow 0)$ transition ionizes the $S = 3/2$ W8 center. The ionization of this center may explain why the $\sim$3.1 eV center can be detected in absorption but not in luminescence. Most probably, the excited electron can escape from the defect and be trapped more efficiently by other defects nearby. The calculated band edge in HSE06 is about 0.2 eV lower than the experimental value, which can naturally account for the inaccuracy of 0.2 eV in the calculated ZPL.

V. SUMMARY

The ground state of Ni_s^- is correctly reproduced by the HSE06 hybrid functional. It is shown to carry a spin $S = 3/2$ in agreement with experiment. The calculated hyperfine couplings support this assignment. Within HSE06 we obtain a triplet state located at 2.0 eV above the valence band in contradiction with an earlier photo-EPR measurement. To confirm the HSE06 results, we performed a G_0W_0 calculation which agrees with the HSE06 results. Photo-EPR experiments need to be reinterpreted in light of these new results. The HSE06 results on the transition levels of substitutional Ni are clearly different than the previous GGA study. The Ni_s^- impurity is shown to be stable for a Fermi energy between 2.36 and 4.66 eV. We calculated the photoexcitation properties of the defect within HSE06. We find a zero phonon line (ZPL) of 2.88 eV with an error of 0.2 eV due to the band gap mismatch of the HSE06 compared to experiment. This ZPL corresponds to the promotion of an electron from the antibonding triplet state to the conduction band. The phonon mode associated with this ZPL is a single triplet mode at 38.4 meV. The only Ni-related center with one phonon mode is the 3.1 eV center measured in absorption. We therefore assign the 3.1 eV center to the Ni_s^-. Using the vacancy model to Ni_s^-, we show that the multielectronic energy levels cannot account for the 2.56 eV center, which is due to another defect than Ni_s^-. According to the 3.1 eV assignment, Ni_s^- can only be seen in absorption. It is therefore not good for quantum information processing, which requires fluorescence property. Further investigations are needed to find the origin of the 2.56 eV ODMR center.

VI. CONCLUSION

Hybrid density functional calculations have been used to characterize the negatively charged substitutional Ni_s^- defect in diamond. The HSE06 functional is shown to reproduce correctly the ground state of Ni_s^- with a total spin $S = 3/2$ localized on Ni and the nearest-neighbor carbon atoms. We unambiguously determine the position of the acceptor level in the gap which is located around 2.0 eV above the valence band maximum and correspond to the antibonding triplet which forms a bound state in the gap due to the strong hybridization between Ni and the nearest-neighbor carbon atoms. We also calculated the excited state properties of Ni_s^-. This defect is proposed to be responsible for the 3.1 eV center measured in absorption experiment. Our results indicate that Ni_s^- might not be an ideal candidate for quantum computing application.

ACKNOWLEDGMENT

We acknowledge the support from the FP7 EU project DIAMANT.

[1] A. M. Zaitsev, in *Handbook of Industrial Diamonds and Diamond Films*, edited by M. Prelas, G. Popovici, and L. Bigelow (Dekker, New York, 1998).
[2] G. Davies, Proc. R. Soc. London Ser. A **348**, 285 (1976).
[3] F. Jelezko and J. Wrachtrup, Phys. Status Solidi A **203**, 3207 (2006).
[4] L. Childress, M. V. G. Dutt, J. M. Taylor, A. S. Zibrov, F. Jelezko, J. Wrachtrup, P. R. Hemmer, and M. D. Lukin, Science **314**, 281 (2006).
[5] R. Epstein, F. Mendoza, Y. Kato, and D. Awschalom, Nat. Phys. **1**, 94 (2005).
[6] R. Hanson, V. Dobrovitski, A. Feigun, O. Gywat, and D. Awschalom, Science **320**, 352 (2008).
[7] L. Jiang, J. M. Taylor, K. Nemoto, W. J. Munro, R. Van Meter, and M. D. Lukin, Phys. Rev. A **79**, 032325 (2009).
[8] F. Jelezko, T. Gaebel, I. Popa, M. Domhan, A. Gruber, and J. Wrachtrup, Phys. Rev. Lett. **93**, 130501 (2004).
[9] P. Neumann, N. Mizuochi, F. Rempp, P. Hemmer, H. Watanabe, S. Yamasaki, V. Jacques, T. Gaebel, F. Jelezko, and J. Wrachtrup, Science **320**, 1326 (2008).
[10] R. Hanson, O. Gywat, and D. D. Awschalom, Phys. Rev. B **74**, 161203(R) (2006).
[11] T. Chanier, C. Pryor, and M. Flatté, Eur. Phys. Lett. **99**, 67006 (2012).
[12] M. Wolfer *et al*., Phys. Stat. Solidi **207**, 2054 (2010).
[13] J. O. Orwa *et al*., J. Appl. Phys. **107**, 093512 (2010).
[14] A. M. Zaitsev, Phys. Rev. B **61**, 12909 (2000).
[15] M. H. Nazaré, A. J. Neves, and G. Davies, Phys. Rev. B **43**, 14196 (1991).
[16] A. T. Collins and H. Kanda, Philos. Mag. B **61**, 797 (1990).
[17] J. Isoya, H. Kanda, J. R. Norris, J. Tang, and M. K. Bowman, Phys. Rev. B **41**, 3905 (1990).
[18] D. M. Hofmann, M. Ludwig, P. Christmann, D. Volm, B. K. Meyer, L. Pereira, L. Santos, and E. Pereira, Phys. Rev. B **50**, 17618 (1994).
[19] R. N. Perreira, W. Gehlhoff, N. A. Sobolev, A. J. Neves, and D. Bimberg, J. Phys.: Condens. Matter **13**, 8957 (2001).
[20] M. H. Nazaré, P. W. Mason, G. D. Watkins, and H. Kanda, Phys. Rev. B **51**, 16741 (1995).
[21] J. P. Perdew, K. Burke, and M. Ernzerhof, Phys. Rev. Lett. **77**, 3865 (1996).
[22] J. Heyd, G. E. Scuseria, and M. Ernzerhof, J. Chem. Phys. **118**, 8207 (2003).
[23] A. V. Krukau, O. A. Vydrov, A. F. Izmaylov, and G. E. Scuseria, J. Chem. Phys. **125**, 224106 (2006).
[24] L. Hedin and S. Lundqvist, in *Solid State Physics*, edited by H. Ehrenreich, F. Seitz, and D. Turnbull (Academic, New York, 1969), Vol. 23.
[25] G. Kresse and J. Furthmüller, Phys. Rev. B **54**, 11169 (1996).
[26] J. Paier *et al*., J. Chem. Phys. **124**, 154709 (2006).
[27] P. E. Blochl, Phys. Rev. B **50**, 17953 (1994).
[28] K. Szász, T. Hornos, M. Marsman and A. Gali (unpublished).
[29] S. O. Kasap and P. Capper, *Springer Handbook of Electronic and Photonic Materials* (Springer, Berlin, 2006), p. 54.
[30] K. Lonsdale, Nature **153**, 22 (1944).
[31] X. Wu, D. Vanderbilt, and D. R. Hamann, Phys. Rev. B **72**, 035105 (2005).
[32] H. J. Monkhorst and J. D. Pack, Phys. Rev. B **13**, 5188 (1976).
[33] J. Zhang, C.-Z. Wang, Z. Z. Zhu, and V. V. Dobrovitski, Phys. Rev. B **84**, 035211 (2011).
[34] T. Chanier, C. Pryor, and M. E. Flatté, Phys. Rev. B **86**, 085203 (2012).
[35] T. Dietl, Phys. Rev. B **77**, 085208 (2008).
[36] T. Chanier, F. Virot, and R. Hayn, Phys. Rev. B **79**, 205204 (2009).
[37] U. Gerstmann and H. Overhof, Physica B **308–310**, 561 (2001).
[38] R. Larico, J. F. Justo, W. V. M. Machado, and L. V. C. Assali, Phys. Rev. B **79**, 115202 (2009).
[39] G. Makov and M. C. Payne, Phys. Rev. B **51**, 4014 (1995).
[40] A. Gali, T. Hornos, N. T. Son, E. Janzén, and W. J. Choyke, Phys. Rev. B **75**, 045211 (2007).
[41] C. W. M. Castleton, A. Höglund, and S. Mirbt, Phys. Rev. B **73**, 035215 (2006).
[42] S. Lany and A. Zunger, Phys. Rev. B **78**, 235104 (2008).
[43] C. Freysoldt, J. Neugebauer and C. G. Van de Walle, Phys. Rev. Lett. **102**, 016402 (2009).
[44] S. E. Taylor and F. Bruneval, Phys. Rev. B **84**, 075155 (2011).
[45] H.-P. Komsa, T. T. Rantala, and A. Pasquarello, Phys. Rev. B **86**, 045112 (2012).
[46] M. Leslie and M. J. Gillan, J. Phys. C **18**, 973 (1985).
[47] A. Gali, E. Janzén, P. Deák, G. Kresse, and E. Kaxiras, Phys. Rev. Lett. **103**, 186404 (2009).
[48] B. K. Ridley, J. Phys. C **13**, 2015 (1980).
[49] G. D. Watkins and P. M. Williams, Phys. Rev. B **52**, 16575 (1995).
[50] M. Lannoo and J. Bourgoin, *Point Defects in Semiconductor I* (Springer, New York, 1981).